

e-Blood

Nodal marginal zone lymphoma: gene expression and miRNA profiling identify diagnostic markers and potential therapeutic targets

Alberto J. Arribas,¹ Yolanda Campos-Martín,¹ Cristina Gómez-Abad,² Patrocinio Algara,¹ Margarita Sánchez-Beato,² María S. Rodríguez-Pinilla,² Santiago Montes-Moreno,³ Nerea Martínez,³ Javier Alves-Ferreira,⁴ Miguel A. Piris,³ and Manuela Mollejo¹

¹Virgen de la Salud Hospital, Toledo, Spain; ²Spanish National Cancer Research Centre, Madrid, Spain; ³Hospital Universitario Marqués de Valdecilla, Instituto de Formación e Investigación Marqués de Valdecilla (IFIMAV), Santander, Spain; and ⁴Hospital Universitario La Paz, Madrid, Spain

Nodal marginal zone lymphoma (NMZL) is a small B-cell neoplasm whose molecular pathogenesis is still essentially unknown and whose differentiation from other small B-cell lymphomas is hampered by the lack of specific markers. We have analyzed gene expression, miRNA profile, and copy number data from 15 NMZL cases. For comparison, 16 follicular lymphomas (FLs), 9 extranodal marginal zone lymphomas, and 8 reactive lymph nodes and B-cell subtypes were included. The

results were validated by quantitative RT-PCR in an independent series, including 61 paraffin-embedded NMZLs. NMZL signature showed an enriched expression of gene sets identifying interleukins, integrins, *CD40*, *PI3K*, *NF-κB*, and *TGF-β*, and included genes expressed by normal marginal zone cells and memory B cells. The most highly overexpressed genes were *SYK*, *TACI*, *CD74*, *CD82*, and *CDC42EP5*. Genes linked to G_2/M and germinal center were down-regulated. Comparison of the

gene expression profiles of NMZL and FL showed enriched expression of *CHIT1*, *TGFB1*, and *TACI* in NMZL, and *BCL6*, *LMO2*, and *CD10* in FL. NMZL displayed increased expression of *miR-221*, *miR-223*, and *let-7f*, whereas FL strongly expressed *miR-494*. Our study identifies new candidate diagnostic molecules for NMZL and reveals survival pathways activated in NMZL. (*Blood*. 2012;119(3):e9-e21)

Introduction

The term marginal zone lymphoma (MZL) encompasses 3 rather unrelated lymphoma subtypes: the extranodal marginal zone lymphoma of mucosa-associated lymphoid tissue (MALT lymphoma), the nodal marginal zone lymphoma (NMZL), and splenic B-cell marginal zone lymphoma (SMZL). In the World Health Organization Classification of Tumors,¹ all 3 types of MZL are considered distinct clinicopathologic entities. NMZL is an uncommon form of small B-cell neoplasm originating in the lymph node, whose morphology resembles lymph nodes involved in MZL of the extranodal or splenic types, but without evidence of extranodal or splenic disease. The relative rarity of NMZLs, which account for fewer than 2% of all lymphoid neoplasms, is a significant obstacle to their molecular investigation.¹ Genomic alterations, including translocations and genomic copy number alterations, are important events in lymphomagenesis,¹ providing diagnostic markers and potential therapeutic targets. However, no characteristic translocations or chromosome imbalances have been described in NMZL. Alterations reported in other MZLs, such as the t(11;18) in MALT-type² and the loss of 7q in SMZL,^{1,3} have not been found in NMZL cases. Only a few cytogenetic alterations of NMZL have been reported, including trisomy 3 in 50% to 70% of cases. More recently, inactivating mutations encoding truncated *A20* proteins have been found in various types of MZL, including 3 of 9 NMZL cases.⁴ *A20* is the protein coded by *TNFAIP3* gene, a negative regulator of NF-κB, located in a frequently lost chromosomal region (6q21-q25).⁴⁻⁶ Other alterations described to date are

rearrangements involving 1p/q, +3/3q, +12, and +18.¹ The absence of molecular or phenotypic markers hinders accurate diagnosis and the differential diagnosis of NMZL from other types of B-cell lymphomas, specifically follicular lymphoma (FL) and reactive lymphoid hyperplasia. Thirteen NMZLs and 8 FLs in this series of cases were included in a previous study by our group that identified *MNDA* as a marker of potential diagnostic value in NMZL.⁷ Some cases of NMZL were classified in the past as monocytoid B-cell lymphomas and linked with the marginal zone.⁸ The normal marginal zone is present in the secondary lymphoid follicles as a concentric area surrounding the mantle follicle and is composed basically of B lymphocytes, macrophages, granulocytes, and dendritic cells that are specialized to capture blood-borne antigens and present them to the resident marginal zone B cells.⁹ The majority of these MZ cells have an IgM^{high}, IgD^{low}, and CD27⁺ phenotype and exhibit somatic hypermutation in their Ig-variable genes, according to the data showing that this zone contains mainly memory B cells.⁹ MZ B cells are involved in early immune response, and the gene expression profile of normal MZ B cells exhibits strong expression of genes, such as *CARD11*, *CXCL12*, *CXCR6*, *TACI*, *MMP12*, *APRIL*, *LTB*, *IFNGR1*, *COL3A1*, *AKAP13*, and *IL2R*.¹⁰

Gene expression profiles (GEPs) have been obtained for other low-grade B-cell lymphomas, such as FL,¹¹ SMZL,¹² and MALT lymphoma.¹³ These gene expression studies have enabled the identification of genes and pathways related to pathogenesis and of

Submitted February 28, 2011; accepted October 16, 2011. Prepublished online as *Blood* First Edition paper, November 22, 2011; DOI 10.1182/blood-2011-02-339556.

The online version of this article contains a data supplement.

The publication costs of this article were defrayed in part by page charge payment. Therefore, and solely to indicate this fact, this article is hereby marked "advertisement" in accordance with 18 USC section 1734.

© 2012 by The American Society of Hematology

Table 1. Clinical characteristics of NMZL patient series

Case no.	Age, y/sex	Clinical stage	HCV	IGHV gene	ID, % homology	Treatment	Outcome (mo)
1	60/F	III	Negative	VH3-33	98.2	CHT	CR (120)
2	80/M	II	ND	VH4-39	94	RT	AWD (64)
3	74/F	I	ND	VH3-72	93	ND	AWD (30)
4	76/F	III	ND	NR	—	CHT	CR (24)
5	73/F	III	Negative	NR	—	CHT	DOD (18)
6	62/F	ND	ND	NR	—	ND	ND
7	65/F	ND	ND	VH4-34/VH3-7	95.9/89.6	ND	ND
8	82/F	III	Negative	VH4-39	92.3	CHT	DXT (54)
9	71/M	IV	Positive	VH3-74	97.3	CHT	AWD (19)
10	76/M	I	ND	VH3-21	93.8	ND	ND
11	55/F	IV	Positive	NR	—	CHT	AWD (34)
12	69/F	III	Negative	NR	—	ND	CR (25)
13	62/M	I	ND	NR	—	RT	CR (46)
14	80/M	IV	ND	VH3-23/VH4b	89.3/91.1	CHT	DXT (13)
15	53/M	IV	ND	VH3-11	89.7	CHT	DOD (7)

NMZL patients had a median age of 68.5 y (range, 53-82 y); 64% of them were women.

ID indicates identity frequency; CHT, chemotherapy; CR, complete remission; ND, not determined; RT, radiotherapy; AWD, alive with disease; NR, no rearrangement; —, not applicable; DOD, dead of disease; and DXT, dead, nonlymphoma-related.

subgroups with distinct pathologic and clinical features and have led to the proposal of new therapeutic targets. However, molecular pathogenesis is essentially unknown in NMZL, and the gene expression profile has yet to be fully described.

miRNAs are 21- to 23-nt-long RNA molecules that regulate the expression of protein-coding genes. More than 700 miRNAs have been identified in mammals and are known to play a role in multiple biologic functions. B-cell differentiation is tightly regulated by miRNAs, and the expression of characteristic sets of miRNAs distinguishes specific stages of B-cell differentiation and B-cell lymphoma main tumor types.^{14,15} The miRNA profile in NMZL has not been described so far, but memory B cells have been shown to display an increased expression of *miR-223*, *miR-146b*, and *miR-150*, and members of the *miR-29* and *miR-181* families and *let-7* cluster, among others.^{15,16}

The aim of this study was to improve our knowledge of the molecular mechanisms involved in NMZL, to find new diagnostic markers of use for its differential diagnosis from other small B-cell lymphomas and reactive therapeutic targets.

Methods

Patients and tissue samples

The series included 15 patients with NMZL. Clinical information about NMZL cases was retrieved from medical records, surgical pathology reports, and the referring clinicians (Table 1). For comparison purposes, we included B-cell subtypes and a set of 33 lymph node samples: 8 lymph nodes with reactive lymphoid hyperplasia (RLN), 5 lymph nodes infiltrated by MALT lymphoma (MZL-MALT), 4 lymph nodes with SMZL, and 16 lymph nodes infiltrated by FL. The criterion for inclusion was the availability of frozen tissue from the diagnostic lymph node specimens in each case. Morphologic examination and CD20 immunostaining revealed the percentage of tumoral cells exceeding 75% in all cases in this study.

To validate the levels of gene expression and miRNA profiles found by microarray analysis, a quantitative RT-PCR experiment was performed with formalin-fixed, paraffin-embedded (FFPE) tissues from an independent series, including 125 cases: 61 NMZL, 57 FL, and 7 RLN.

All cases were selected from the routine and consultation files of the Pathology and Genetics Laboratories of the Virgen de la Salud Hospital (HVS, Toledo, Spain), the Spanish National Cancer Research Center (Madrid, Spain), and the Spanish Tumor Bank Network. Cases were

diagnosed on the basis of morphology, immunophenotype, and molecular findings according to the World Health Organization classification criteria.¹ Research was performed under the supervision of the Institutional Review Board of the HVS, Toledo, Spain.

Selection of B-cell subsets

B-cell populations were obtained by magnetic cell separation from 6 patients undergoing routine tonsillectomy. The germinal center (GC) B cells were recognized by CD38^{high} IgD⁻, CD27⁺, and CD10⁺ expression, whereas memory B cells were isolated by stainings with CD38^{low}, CD27⁺, IgD^{low}, and CD10⁻. The complete procedure for isolating B-cell subsets is described in supplemental Material 1 (available on the *Blood* Web site; see the Supplemental Materials link at the top of the online article).

RNA and DNA isolation

For GEP and miRNA hybridization, total RNA was isolated from each B-cell subset, 40 frozen tumoral blocks and 8 control samples from RLN by TRIzol Reagent (Invitrogen) following the manufacturer's recommendations. The quality of the RNA produced was checked by 1% agarose electrophoresis. Cases with poor-quality RNA were discarded.

Copy number alteration (CNA) was assayed with the DNA from 15 NMZL of frozen-tissue cases, extracted using the standard phenol-chloroform protocol.

Microarray procedures: GEP, miRNA, and CNA hybridization

RNA for GEP was hybridized on a Whole Human Genome Agilent 4 × 44K Oligonucleotide Microarray (Agilent Technologies) as reported.¹⁷

The miRNA microarray experiments were done using the Agilent Human miRNA Microarray (V1), 8 × 15K (Agilent Technologies). For each tissue sample, 100 ng total RNA was hybridized with the miRNA array and further processed as previously described.¹⁸

For CNA, the DNA was hybridized on an Agilent Human Genome CGH Microarray Kit 4 × 44K (Agilent Technologies) as described.¹⁹ Human female- and male-pooled gDNA (Promega) was used to normalize the comparative genomic hybridization (CGH) results. Results were considered valuable in 14 cases. The samples (1 μg DNA) were labeled with Cy5, and the DNA donor pool was labeled with Cy3. The commonly affected regions were compared with the Database of Genomic Variants (<http://projects.tcag.ca/variation>): regions with an overlap of more than 80% between probes and known copy number variations were considered bona fide copy number variations and excluded from further analysis.

All microarray data can be viewed at the Gene Expression Omnibus under the following accession numbers: superseries data under accession

number GSE32233, gene expression data under GSE32231, miRNAs data under GSE32232, and CGH data under GSE32436.

Microarray data analysis: GEP, miRNA, B-cell subsets

The background subtraction of microarray data was carried out using GEPAS Version 4.0 (<http://gepas.bioinfo.cipf.es>). The dataset was normalized by lowess within-array normalization and quantile between-array normalization, and then preprocessed.

We used ANOVA and *t* tests (<http://pomelo2.bioinfo.cnio.es/>) to compare the expression of the NMZL gene and miRNA signatures with that of the RLN, with the other MZL subtypes (SMZL and MALT lymphoma) and FL. In all these comparisons, the genes and the miRNAs with false discovery rate (FDR) < 0.05 were considered significant.

The *t* statistic in gene set enrichment analysis (GSEA; <http://www.broad.mit.edu/gsea/>) was calculated to identify the pathways and functional groups enriched in the NMZL signature. The GSEA gene sets used were selected from a curated version of Biocarta, KEGG, and CCG pathway databases, as previously described.²⁰ The gene sets with values of *P* < .05 and FDR < 0.25 were considered to be enriched and potentially relevant in each case.

CNA was normalized using CAPweb Version 2.0²¹ from the Curie Institute (<http://bioinfo-out.curie.fr/CAPweb>).

miRNA target prediction and miRNA target correlation

We followed the previously described procedure²² to identify associations between differentially expressed miRNAs (FDR < 0.05) and gene expression signatures (FDR < 0.05). The GSEA (Pearson correlation) was used to test the enrichment of gene sets related to each corresponding miRNA. Those with values of *P* < .05 and FDR < 0.25 were considered to be enriched in each case.

Quantitative real-time RT-PCR analysis

To validate GEP and miRNA microarray data, we carried out a quantitative RT-PCR assay. Total RNA was extracted from FFPE sections of an independent patient group following the manufacturer's instructions using an miRNeasy FFPE Kit (QIAGEN).

Quantitative RT-PCR experiments were performed on selected genes, on the tested miRNAs, and on each B-cell subset using TaqMan probes (Applied Biosystems) as previously described.^{12,22} The relative degree of change for each gene and miRNA was calculated using the $RQ = 2^{-\Delta Ct}$ method (for GEP $\Delta Ct = (C_{t_{gene}} - C_{t_{GAPDH}})$ and for miRNAs $\Delta Ct = (C_{t_{miRNA}} - C_{t_{U6}})$) with *GAPDH* as the GEP endogenous control and *RNU6B* as the miRNA endogenous control. *C_t* values of at least 36 were considered beyond the limit of detection.

The *t* test and one-way ANOVA (SPSS Version 17.0) were used, and the genes and miRNAs with values of *P* < .05 were considered significant.

Immunostaining techniques

A series of FFPE were analyzed using IHC by staining 2- to 4- μ m-thick sections, following the Dako EnVision FLEX procedure (Dako Denmark). Some of the most relevant genes in the assay, such as *CD82*, *TACI*, *CD44*, *CHIT1*, *TOM1*, and *LASS4*, were studied by IHC. The antibodies used are detailed in (supplemental Table 8).

For immunohistochemical evaluation, cases were scored semiquantitatively, with respect to the number of positive cells and the intensity of the expression. Antibodies producing inconsistent or unreliable results were not quantified. Cases were considered as CD44-positive and LASS4-positive if these markers were expressed in more than 50% of tumoral cells at an intermediate-high intensity, and for CHIT1 when immunostaining was present in more than 10% of macrophage cells.

Results

Nodal marginal zone signature

We have characterized the protein-coding genes and miRNA signature for NMZL and selected B-cell populations. The expression of selected protein-coding genes and miRNAs was validated in a large independent FFPE series by quantitative RT-PCR. Putative targets for the miRNAs were also identified.

Gene expression profiling

Unsupervised hierarchical clustering revealed a relatively homogeneous profile for the entire series, whereby most NMZL, FL, and RLN cases were clustered in well-separated groups (supplemental Figure 1). The expression profiles of lymph nodes infiltrated by NMZL, MZL-MALT, and SMZL were compared statistically revealing no differentially expressed genes, although the analysis of these data should take into consideration the small number of lymph nodes involved in MZL-MALT and SMZL available for study.

Supervised hierarchical clustering identified an NMZL signature containing 264 up-regulated genes and 184 down-regulated genes (Figure 1). The most relevant significantly deregulated genes in the NMZL signature are shown in Table 2 and Figure 1 (complete NMZL signature in supplemental Table 1). The 10 most up-regulated genes were *SYK*, *TACI*, *CD74*, *CD82*, *CDC42EP5*, *TFEB*, *LYN*, *UCP2*, *ACP5*, and *HLA-DMA*. Among the most underexpressed genes were those associated with proliferation and cell cycle (*PBK*, *CD2AP*, and *CDC7*), DNA repair (*RAD54B*, *PSMC3IP*, *MSH2*), GC (*CD10*), meiosis (*MND1*, *MNS1*), chromatin modification (*HDAC2*), cell apoptosis (*BNIP3*, *IKIP*), and extracellular matrix and cell adhesion (*ANXA1*, *LMO7*).

GSEA revealed enriched pathways in NMZL compared with RLN, including IL6, integrins, IL2RB, CD40, RAC-CYCD, TGF β , PTDINS (PIK3C2A), IL2, RELA, and TNFR1 gene sets (Figure 2; Table 3).

miRNA profiling

The *t* test showed 4 miRNAs to be significantly deregulated in NMZL compared with RLN: 3 of them were up-regulated (*miR-221*, *miR-555*, and *miR-29c*) and one was down-regulated (*miR-532-5p*; Table 4; Figure 3; supplemental Figure 3). The prediction targets for *miR-221* and *miR-555* included the repressed genes *LMO2* and *CD10*, whereas *miR-532-5p* showed targets in the up-regulated *SYK*, *LYN*, and *RELA* genes.

The results detailing the relationship between gene sets and miRNAs are shown in supplemental Material 2.

NMZL versus FL

The differential diagnosis of NMZL and FL is not always clear. The microarray data from frozen tissues in 15 samples of NMZL and 16 of FL were used to compare NMZL and FL gene expression and miRNA profiles. The correlation between miRNAs and gene targets was also investigated.

Supervised hierarchical clustering highlighted a list of interesting deregulated genes. NMZL cases had increased expression of *CHIT1*, *TACI*, *TRAF4*, *TGFB1*, *CD82*, *PTPN1*, and *CD44*. Conversely, FL cases were characterized by the increased expression of a series of GC markers, including *CD10* (*MME*), *BCL6*, *GCET1* (*SERPINA9*), and *LMO2*, whereas genes that are normal marginal

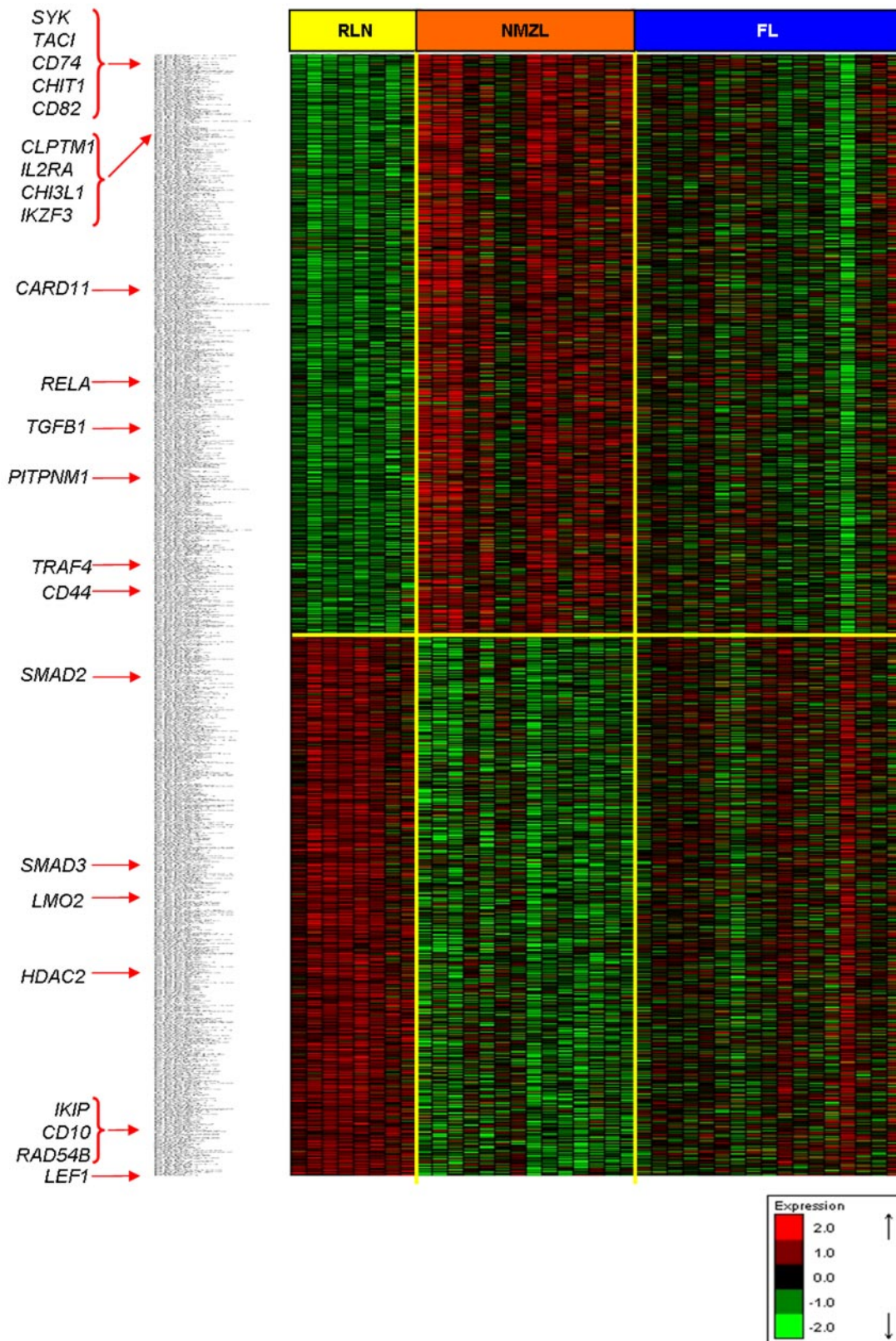


Figure 1. NMZL gene expression signature. Hierarchical clustering of genes with FDR < 0.10 in NMZL versus RLN *t* test comparison. Some relevant genes of the signature are marked with red arrows. Red and green represent high- and low-level expression, respectively.

zone-related, such as *TAC1* and *CD44*, were up-regulated in NMZL. Furthermore, NF-κB-related and binding genes (*TRAF4*, *CD82*, *CLIC1*, *CSNK2B*, and *VARS*) were up-regulated in NMZL.

In the same way, *IL32*, histones (some isoforms of *HIST1H* and *HIST2H*), *TNF* family members (*TAC1*, *TNFRSF14*), and regulatory genes involved in lymphocyte activation, such as *CLPTM1*

Table 2. NMZL gene expression signature: most relevant NMZL signature genes

Gene	NMZL vs RLN comparison		NMZL vs FL comparison		Memory vs GC comparison		Cytoband	Description
	Fold change	FDR	Fold change	FDR	Fold change	P		
<i>TACI</i> *	2.075	0.032	1.987	0.042	0.925	< .001	17p11.2	TNF receptor, B-cell stimulation. NF- κ B activator
<i>CHIT1</i> *	2.044	NS (0.072)	2.527	0.020	-0.234	NS	1q31-q32	Microenvironment involved
<i>CD82</i> *	2.045	0.012	1.727	0.027	0.399	NS	11p11.2	Coactivator for the BCR pathway
<i>CHI3L1</i>	1.588	0.028	1.635	0.029	0.133	ND	1q32.1	Microenvironment involved
<i>CLPTM1</i>	1.652	0.009	1.334	0.049	0.249	ND	19q13.32	Lymphocyte activation
<i>PTPN1</i>	1.487	0.008	1.243	0.026	0.245	ND	20q13.13	Signal transduction
<i>TRAF4</i>	1.036	0.033	1.139	0.022	-0.110	ND	17q11.2	TNF receptor-associated factor; NF- κ B activation
<i>TGF-β1</i> *	1.175	0.010	1.009	0.025	0.371	NS	19q13.2	Cell proliferation and differentiation
<i>CD44</i> *	0.874	0.029	1.285	0.006	1.131	NS	11p13	Adhesion molecule related to marginal zone
<i>SMAD2</i>	-0.837	0.010	-0.712	0.030	0.000	ND	18q21.1	TGF- β signaling pathway
<i>HDAC2</i>	-1.258	0.007	-1.016	0.013	-0.171	ND	6q22.1	Chromatin modification
<i>IKIP</i> *	-1.428	0.029	-1.270	0.045	-0.179	ND	12q23.1	Apoptosis
<i>RAD54B</i> *	-1.775	0.007	-1.291	0.026	-0.241	NS	8q22.1	DNA repair
<i>SMAD3</i>	-2.447	0.029	-1.226	0.044	0.335	ND	6q23.1	TGF- β signaling pathway
<i>LMO2</i> *	-2.533	0.006	-1.732	0.014	-0.545	NS	11p13	GC marker
<i>LEF1</i>	-2.828	0.009	-1.768	0.021	1.682	ND	4q25	Implicated in gene expression transcription
<i>CD10</i>	-4.269	0.006	-2.172	0.041	-0.612	ND	3q32.31	GC marker

Fold changes corresponding to the log₂ difference between the NMZL and RLN, NMZL, and FL, and memory B-cell and GC B-cell averages, respectively. FDR and P values are from the *t* test (<http://pomelo2.bioinfo.cnio.es/>).

NS indicates not significant; and ND, not determined.

*To validate the microarray data, the gene was included in the quantitative RT-PCR assay.

and *TGFB1*, were more highly expressed in NMZL than in FL (Table 2; Figure 1; supplemental Table 2).

GSEA analysis revealed enriched pathways related to memory B cells (IgM⁺ IgD⁻ CD27⁺) in NMZL compared with FL. We also found the *IL10* pathway to be strongly represented in NMZL. Genes linked to the GC were up-regulated in FL (Figure 4).

miRNAs differentially expressed between NMZL and FL were also investigated, revealing 61 deregulated miRNAs: 24 were up-regulated and 37 were repressed in NMZL (Table 4; Figure 3; supplemental Table 3). Some of the up-regulated miRNAs were *miR-223* and *let-7f*, whose putative targets are *LMO2* and cell cycle-related genes, respectively. The functional relationship between *miR-223* and *LMO2* in B cells has already been demonstrated.¹⁶ The *let-7* cluster, including *let-7f* miRNA, is involved in cell cycle regulation and cell division.²³ The miRNAs down-regulated in NMZL included *miR-494*, *miR-765*, *miR-370*, *miR-30d*, *miR-181a*, and *miR-29b*. The miRNAs *miR-370* and *miR-765* have the *TRAF4* and *TGFB1* genes as their respective potential targets. *CCND2* is a putative target of *miR-494* according to the TargetScan algorithm.

NMZL homology with memory B cells

To determine whether NMZL signature has homology with the gene expression patterns of the normal memory B-cell subpopulation, we identified the GEP and miRNA profile of memory B cells and GC B cells. The comparison of the GEP and miRNAs of memory and GC B cells is presented in supplemental Tables 6 and 7.

The most relevant genes and miRNAs that are up-regulated in NMZL cells, including *TACI*, *CD44*, *let-7* family members, and *miR-223*, have been previously described in memory B cells,^{10,13,15,24} whereas the GC B cells showed overexpression of GC markers, such as *CD10*, *BCL6*, and *LMO2* and the miRNAs *miR-28* and *miR-17-5p*, among others. Thus, protein-coding genes and miRNA profiles of NMZL both reproduced the findings obtained for memory B cells, which is consistent with the data showing that memory B cells are the predominant cell population in the human normal marginal zone.²⁴

Validation of microarray data in an independent FFPE series

Microarray results were validated by quantitative RT-PCR and IHC assays in an independent FFPE series. The set of genes selected for validation by quantitative RT-PCR was a combination of those differentially expressed genes that were common in NMZL against RLN and opposite FL comparisons, including *TACI*, *CHIT1*, *CD82*, *TGFB1*, *CD44*, *IKIP*, *RAD54B*, and *LMO2* (Table 2). The selected miRNAs for validation were those with higher differential expression between NMZL versus RLN and NMZL versus FL (Table 4). The genes with higher differential expression between NMZL versus RLN were selected for confirmation by IHC assay (Table 2).

The quantitative RT-PCR analysis showed higher expression levels in NMZL versus FL and versus RLN of *TACI* and *CHIT1* and a lower level of *LMO2* and *RAD54B*, with significant P values for all genes. The complete results are shown in Figure 5A. The data for *IKIP* could not be evaluated because the TaqMan probe was not amplified. The differential expression of *miR-221*, *miR-223*, *let-7f*, and *miR-494* was also confirmed (Figure 5B). Quantitative RT-PCR failed to confirm the results concerning *miR-29c*. Data for the miRNAs not shown in Figure 5B could not be evaluated. The results of the ANOVA for the most relevant genes and the miRNAs in the assay are shown in supplemental Table 4. The lack of validation for some genes and miRNAs may be the result of the relatively few cases of RLN in the FFPE series.

CD44 protein expression was significantly higher in the NMZL cases than in FL (*P* = .0157); thus, CD44 was positive in 90% of the NMZL cases but was only expressed in 69% of FL cases. CHIT1 expression, present in macrophages but not in the tumoral cells, was stronger in NMZLs (48%) than in FLs (38%), although this difference was not statistically significant (Figure 6; supplemental Table 8).

Thus, the validation of the NMZL versus RLN comparison was corroborated in 4 of 7 genes (*TACI*, *CHIT1*, *LMO2*, and *RAD54B*) and 1 of 2 miRNAs (*miR-221*). The NMZL versus FL assay was validated in all genes (7 of 7) and all miRNAs (4 of 4): *miR-223*, *let-7f*, *miR-221*, and *miR-494*. Finally, *CD44* was not validated in the NMZL versus RLN comparison by RT-PCR, although it was using IHC.

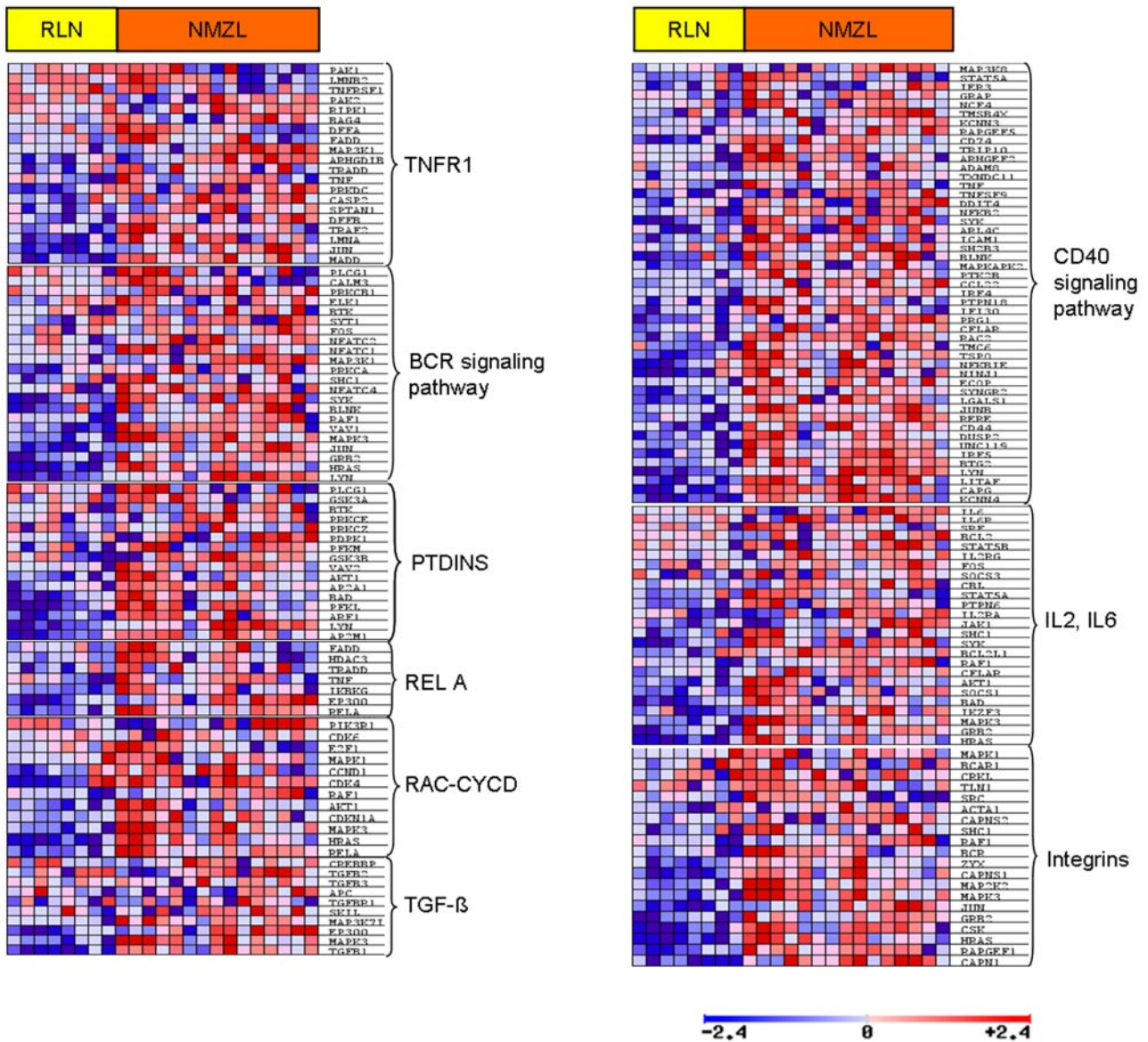


Figure 2. Gene set and pathways enriched in NMZL. The expression of genes representing different B-cell pathways by GSEA analysis (*t* test). Red and blue represent higher and lower expression, respectively.

CNAs

Details of the CNA analysis are shown in supplemental Table 5 and supplemental Figure 3. This assay revealed gains at various chromosomal sites where we studied the relationship between the CNA and GEP data (Table 5; Figure 7). We found miRNAs belonging to the NMZL signature in several of these gained bands. We also observed a very low frequency of CNA losses.

Discussion

The diagnosis of NMZL is still hampered by the lack of consistent, specific markers. Here we have analyzed the gene expression profile and copy number in a series of cases selected using very conservative diagnostic criteria that excluded all cases with intermediate features or insufficient clinical data. This reduced the number of cases that could be analyzed but improved the chance of identifying specific immunohistochemi-

cal or molecular markers. The gene expression profiles were very similar throughout the NMZL series, which guarantees the homogeneity of data and suggests that NMZL is a unique entity.

The NMZL gene expression profile identified in this way encompasses pathways and genes of the normal marginal zone and memory B cells, the cell subpopulation that occupies the normal marginal zone.²⁴ These findings confirm that NMZL is the tumoral counterpart of marginal zone cells. This corroborates previous observations mainly based on the morphologic analysis of MZL and suggests that typical MZL cases could be more homogeneous than previously thought.

The gene expression profile of all MZL subtypes described to date^{12,13,25,26} suggests that chronic antigenic stimulation, potentially originating from pathogenic organisms or arising from autoimmune disorders, has an important role in the ontogeny of these tumors. The inflammatory microenvironment, composed of proinflammatory cytokines and cells including antigen-presenting cells and T cells, seems to be crucial in these different lymphoma types.

Table 3. GSEA for NMZL gene expression profile

Gene sets	P	FDR	Up-regulated genes
IL6 pathway	.004	0.177	SHC1, JAK1, CSNK2A1, RAF1, STAT3, JUN, HRAS, MAPK3, GRB2
Integrin pathway	.006	0.135	BCR, RAF1, ZYX, JUN, CAPNS1, CSK, MAP2K2, HRAS, MAPK3, GRB2, RAPGEF1, CAPN1
IL2RB pathway	.004	0.152	SHC1, PTPN6, IL2RA, JAK1, SYK, RAF1, CFLAR, SOCS1, BAD, AKT1, BCL2L1, HRAS, MAPK3, IKZF3, GRB2, CSNK2A1, JUN
CD40 signaling during GC development	.028	0.202	KCNN4, BTG2, CAPG, LYN, LITAF, IRF5, DUSP2, JUNB, CD44, IRF4, CD74, NF-KB2, IFI30, ADAM8, TNF
RAC and CYCD pathway	.021	0.210	RELA, HRAS, MAPK3, CDKN1A, AKT1, RAF1, CDK4
TGF-β pathway	.023	0.210	MAP3K71P1, EP300, MAPK3, TGF-β1
PTD INS pathway	.028	0.195	PFKM, GSK3B, VAV2, AP2A1, BAD, AKT1, PFKL, ARF1, AP2M1, LYN
IL2 pathway	.030	0.197	SHC1, PTPN6, IL2RA, JAK1, SYK, RAF1, CFLAR, SOCS1, BAD, AKT1, BCL2L1, HRAS, MAPK3, IKZF3, GRB2, CSNK2A1, JUN
RELA pathway	.042	0.203	RELA, EP300, IKBKG, TNF, HDAC3, FADD, TRADD
TNFR1 pathway	.023	0.214	MADD, JUN, LMNA, DFFB, SPTAN1, CASP2, PRKDC, TNF, TRADD, ARHGDI1, MAP3K1, FADD

The gene sets were considered up-regulated values of $P < .05$ and $FDR < 0.250$ in GSEA analysis using a t test.

Remarkably, in this NMZL series, the GSEA analysis found up-regulation of the *IL6* and *IL2* cytokine pathways, and *CD40* signaling, which are involved in B-cell survival. Other up-regulated cytokines, such as *IFN-γ* and *CD70* (*CD27L*), also appear in the NMZL signature. Accordingly, inflammatory cytokines present in the microenvironment might contribute to the onset and progression of lymphoma or at least contribute to the survival of tumor cells. The overexpression of genes functionally related to processes of antigen presentation, such as class I and class II *HLAs*, and other structurally related genes, such as *CD81* and *CD74*, suggests an important role of the immune response in this lymphoma. *CD74* is critical to MHC class II antigen processing and has been proposed as a candidate target for the immunotherapy of B-cell neoplasms by Stein et al.²⁷ This chaperone was shown to be directly involved in the maturation of B cells through a pathway involving *NF-κB*.²⁸

TAC1 (*TNFRSF13B*), a transmembrane activator and CAML interactor, is a *TNF* family receptor involved in the TI-2 response for the efficient differentiation from marginal zone B cells to plasma cells.²⁹ *TAC1* has multiple functions in the B cell, apoptosis regulation, and *NF-κB* canonical and noncanonical (through recruitment of *TRAF2*, *TRAF5*, and *TRAF6*) activation.³⁰ Therefore, *TAC1* should be considered an important gene in the molecular mechanism of NMZL and could be a new candidate for diagnosis and as a therapeutic target. The splenic marginal zone is essential for an

appropriate TI-2 immune response, with absence or dysfunction of the spleen, resulting in an increased risk of infection by pathogens with polysaccharide capsule.³¹ Transforming growth factor β-1 (*TGFβ1*) is a member of the *TGF-β* superfamily, which plays a crucial role in regulating the balance between proliferation and differentiation in hematopoietic cells.³² *TGFβ1* has been ascribed context-dependent³³ contrary functions in hematopoietic cells, with respect to growth inhibition and tumor progression. Increased *TGFβ1* signaling, as seen in NMZL cases, is an indication of the role that other cell subpopulations, macrophages, regulatory T cells, and other cells could play in NMZL pathogenesis.³³

Antigen stimulation and selection of neoplastic cells are thought to occur in gastric MALT lymphoma and SMZL.^{12,13} At present, the role of antigen stimulation in NMZL is unclear, although association with hepatitis C virus (HCV) has been described in a highly variable proportion of cases.³⁴ The small number (2) of HCV-positive cases in our series prevents any firm conclusion being drawn, but the up-regulation of surface molecules and genes functionally related to antigen-presenting processes suggests that antigen stimulation may play a crucial role in the pathogenesis of this lymphoma. *CD81* has been described as being an HCV receptor³⁵ and was up-regulated in the HCV-positive cases.

In addition, the data obtained here seem to identify signaling from *BCR* and coregulated receptors as being essential for NMZL

Table 4. NMZL miRNA signature

Gene	NMZL vs RLN comparison		NMZL vs FL comparison		Memory vs GC comparison		Cytoband	CNA*	Putative prediction targets
	Fold change	FDR	Fold change	FDR	Fold change	P			
<i>miR-223</i>	0.298	NS	0.978	0.009	1.023	NS (.054)	Xq12	—	<i>LMO2, MYBL1</i>
<i>miR-29c</i>	0.809	0.031	0.188	NS	1.081	< .001	1q32.2	—	<i>PTEN, PLAG1, GNB4, MEST</i>
<i>miR-221</i>	0.562	0.002	0.430	0.009	1.057	NS	Xp11.3	Gain	<i>CD10, LMO2</i>
<i>miR-34a</i>	0.432	NS	0.494	0.024	0.992	ND	1p36.22	Gain	<i>LEF1, LASS6, GRSF1, E2F3</i>
<i>let-7f</i>	0.109	NS	0.809	0.008	1.020	< .05	9q22.32	—	<i>SMAD2, LBR, CCDC100</i>
<i>miR-625</i>	0.396	0.092	0.447	0.002	1.010	ND	14q23.3	—	<i>PAG1, SFRS1, BAT3, ABCF3</i>
<i>miR-222</i>	0.330	NS	0.052	NS	1.025	ND	Xp11.3	Gain	<i>MYO10</i>
<i>miR-202</i>	0.320	NS	-0.036	NS	1.045	ND	10q26.3	Gain	<i>MYCBP, LEPROTL1, STX17</i>
<i>miR-765</i>	-0.207	NS	-1.491	0.000	0.990	ND	1q23.1	—	<i>TGF-β1</i>
<i>miR-370</i>	-0.221	NS	-1.961	0.000	0.960	ND	14q32.2	—	<i>TRAF4</i>
<i>miR-513</i>	-0.230	NS	-2.226	0.000	0.939	ND	Xq27.3	—	<i>DRAP1, SMARCA1, HMGB1</i>
<i>miR-494</i>	-0.937	NS	-2.969	0.000	0.989	< .001	14q32.31	—	<i>CCND2, ASL, PMPCA, BCL6</i>

Most relevant miRNAs with significantly differential expression in comparisons of NMZL and RLN, NMZL and FL, and of memory B cells versus GC B cells. Fold changes correspond to the log2 difference between averages. FDR and P values are from the t test (<http://pomelo2.bioinfo.cnio.es/>). To validate the microarray data, all miRNAs in this table were included in the quantitative RT-PCR assay. Only 5 miRNAs had valuable data in the quantitative RT-PCR assay (C_t value > 36): *miR-223*, *miR-29c*, *miR-221*, *let-7f*, and *miR-494*.

NS indicates not significant; —, not applicable; and ND, not determined.

*Chromosomal sites with alterations in the CGH microarray data.

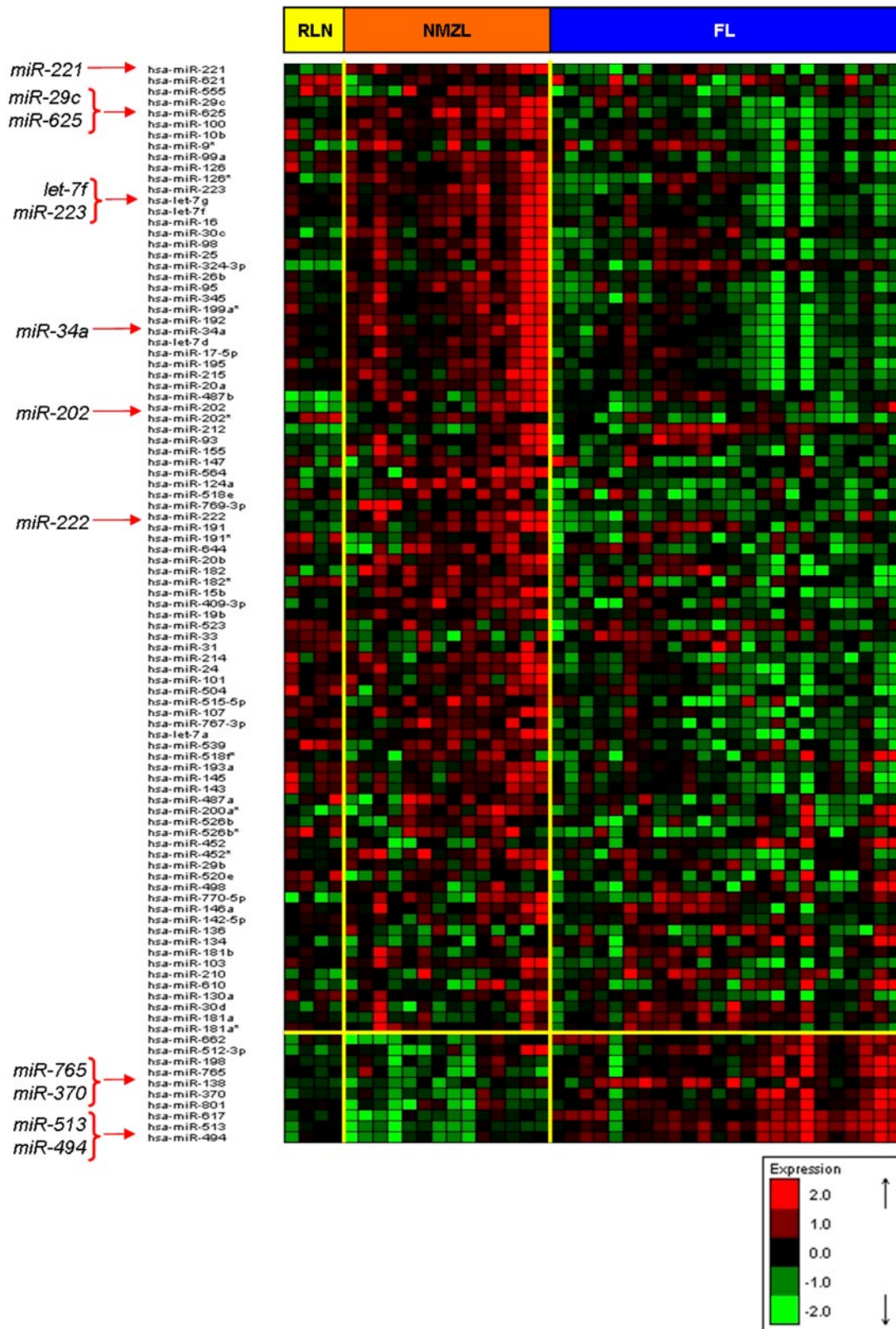


Figure 3. NMZL miRNA signature. Hierarchical clustering of miRNAs with FDR < 0.05 in ANOVA (NMZL vs RLN vs FL) and *t* test comparison. Some important miRNAs in the signature are marked with red arrows. Red and green represent high- and low-level expression, respectively.

survival. *SYK*, *LYN*, *BLK*, and *BLNK* are tyrosine kinases involved in the *BCR* signaling pathway, which is also known to be overexpressed in other MZLs.^{12,13}

In the molecular signature of NMZL, we found a large number of overexpressed genes associated with *NF-κB* signaling pathway, such as *CD74*, *CD81*, *CD82*, *RELA*, and *TRAF4*, thus extending

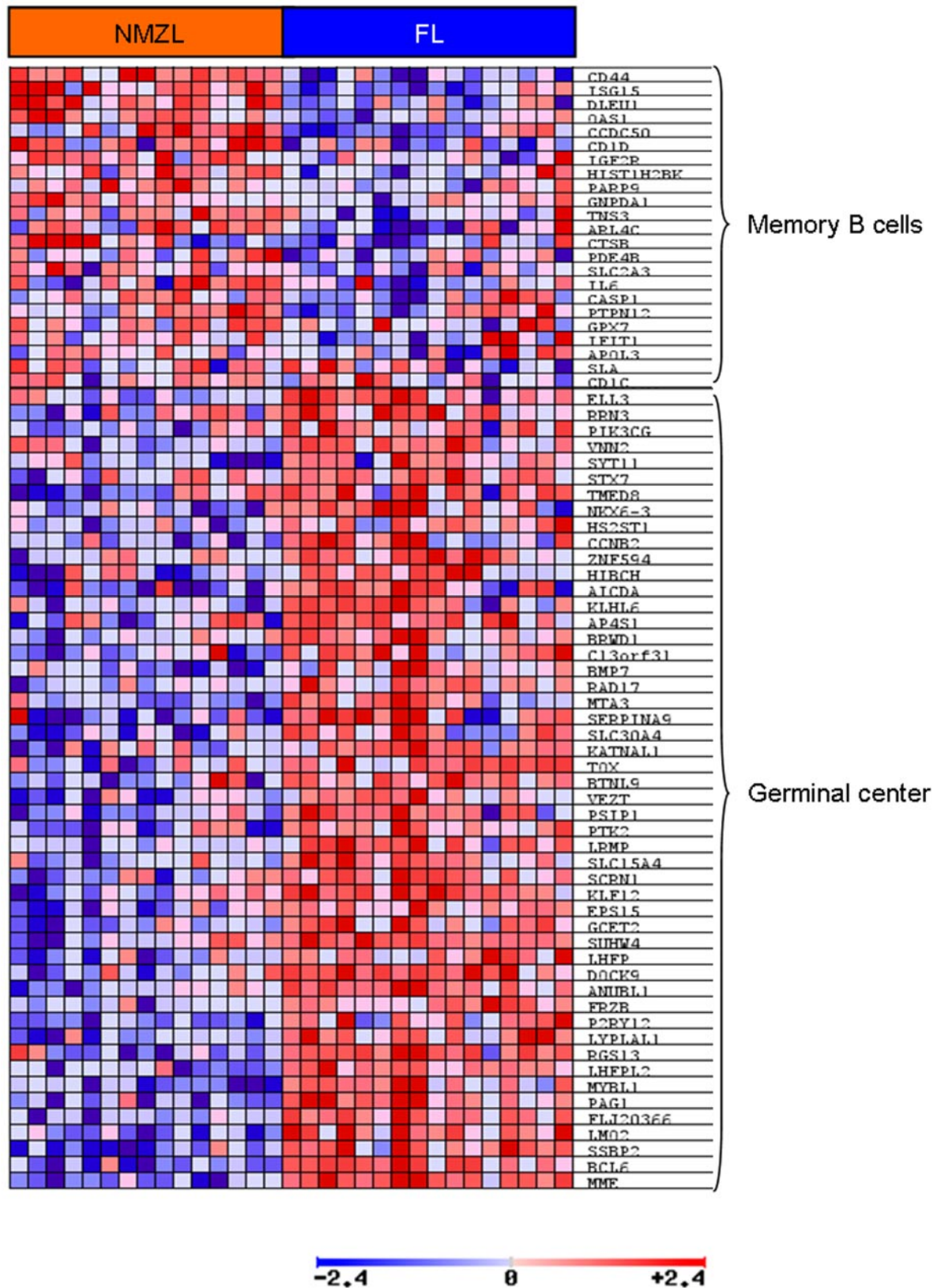


Figure 4. B cell signature expression in NMZL and FL. The GSEA assay revealed up-regulation of genes related to the germinal center were overexpressed in FL cases. Red and blue indicate higher and lower expression, respectively.

and confirming the role of this transcription factor in lymphoma pathogenesis.^{7,36} Neither copy number nor expression profiling data in this study confirmed previous findings concerning the frequent loss of *TNFAIP3* in NMZL.⁷

The NMZL cases overexpressed marginal zone-like genes, such as *CD44* and *TAC1*, genes of diagnostic value for NMZL, such as *MNDA*, and other relevant genes, including *CHIT1*. Expression of *MNDA* protein was previously evaluated by our group and found to

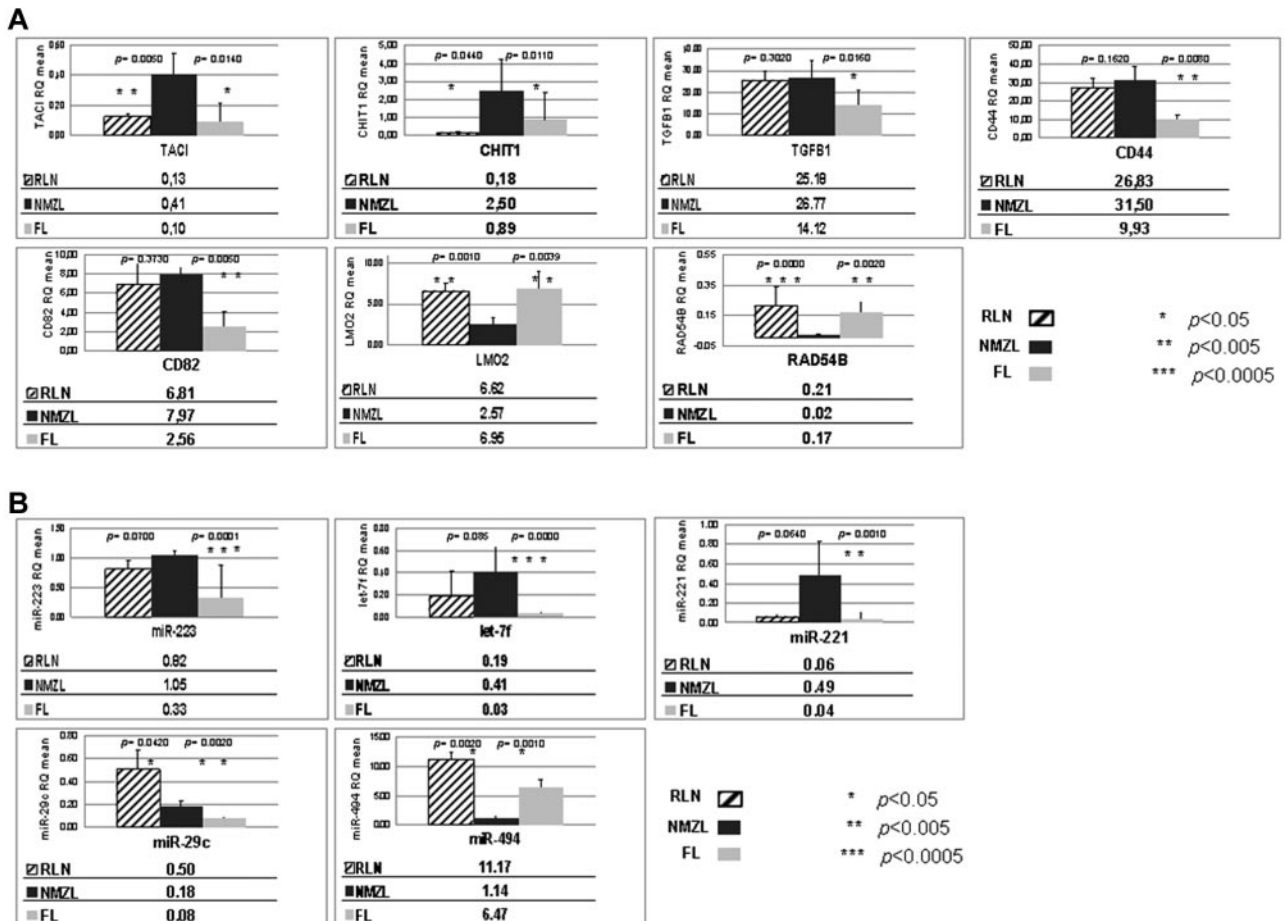


Figure 5. Quantitative RT-PCR assay. (A) Quantitative RT-PCR assay for GEP. (B) Quantitative RT-PCR study for miRNAs. Expression data (RQ mean) of the validated quantitative RT-PCR genes and miRNAs included in the NMZL signature compared with RLN and FL. RQ values are shown below the corresponding graph, and the *t* test (*P*) values are shown on the bars for each comparison. The genes and miRNAs that appear in Tables 2 and 4 (and that are not shown in Figure 5) had no valuable data in the quantitative RT-PCR assay (*C_t* values > 36): *IKIP* gene and *miR-34a*, *miR-625*, *miR-222*, *miR-202*, *miR-765*, *miR-370*, and *miR-513*. Oblique striped represent RLN cases; black, NMZL cases; and light gray, FL cases.

be significantly higher in NMZL than in FL. The FL samples strongly expressed known GC markers, such as *CD10*, *BCL6*, and *LMO2*. *CD44* is an adhesion molecule expressed in MZLs and other non-Hodgkin lymphomas and is an integral member of the *CD74* receptor complex.^{25,37} The increased expression of chiotridisidase-1 or chitinase-1 (*CHIT1*), a marker of macrophages, in the NMZL cases highlights the

essential role of specific subpopulations of accompanying cells in the normal and neoplastic marginal zone.³⁸ A previous independent study found *TACI* protein expression to be higher in NMZL than in FL.³⁹ *TACI*, *CHIT1*, and *TGFB1* showed stronger expression, with microarrays and RT-PCR, in NMZL than FL and could be candidates for novel diagnostic markers in NMZL.

Table 5. Chromosomal band gains and losses by CGH microarray

Band	Imbalance	Frequency, no. (%)	Genes involved*
22q13.32-33	Gain	8/14(67)	<i>CHKB</i> , <i>SBF1</i>
14q32.33	Gain	5/14(36)	—
Xq28	Gain	5/14(36)	<i>TAZ</i>
10q26.13	Gain	4/14(29)	—
16p13.3	Gain	4/14(29)	<i>RHOT2</i> , <i>RAB40C</i>
17q25	Gain	4/14(29)	<i>SYNGR2</i> , <i>WBP2</i>
16q21-24	Gain	3/14(21)	<i>PLCG2</i>
1p36	Gain	2/14(14)	<i>MIB2</i> , <i>SDF4</i>
6p21.33	Gain	2/14(14)	<i>HLA-DMA</i> , <i>HLA-E</i> , <i>HLA-H</i> , <i>HLA-A</i> , <i>HLA-B</i>
6p22.1	Gain	2/14(14)	<i>HIST1H2</i> cluster
8q24.3	Gain	2/14(14)	—
Xp11.23	Gain	2/14(14)	<i>OTUD5</i>
11p15.5	Gain	2/14(14)	<i>IFITM</i> family genes
22q11.21	Loss	2/14(14)	<i>PRAME</i> ; described as a polymorphism resulting from CNV_53983, CNV_35989, and CNV_53720

— indicates not applicable.

*Data are the deregulated genes located in the corresponding cytoband. The deregulated genes belong to the NMZL signature (FDR < 0.05 in the NMZL vs RLN comparison, all NMZL cases included).

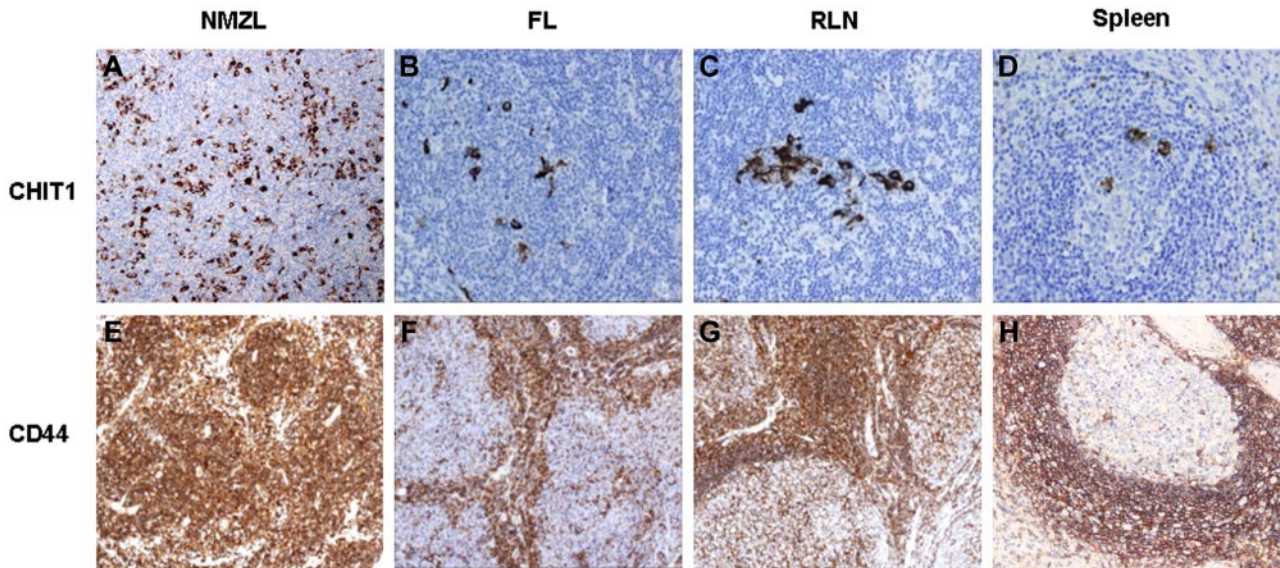


Figure 6. IHC tissue staining. NMZL, FL, and RLN differential expression data revealed by IHC. Examples of cases immunostained for *CHIT1* and *CD44*. All images were acquired using an Olympus A×80 microscope (Olympus) with a magnification 400×, captured with an Olympus DP72 3.0 camera and processed with Cell A software (Olympus Soft Imaging Solutions, Version 3.29).

Data obtained suggest that the differential expression of *miR-221* in NMZL against RLN, and *miR-223*, *let-7f*, and *miR-494* in NMZL versus FL could be of potential diagnostic value. FL and GC cells are distinguished by an increased expression of *LMO2*, and a diminished expression of *miR-223*. *LMO2* targeting by *miR-223* is essential to the regulation of B-cell development.¹⁶ The data here obtained showing *LMO2* down-regulation and increased *miR-223* expression suggest that this relation could also play a role in NMZL. *Let-7* cluster is implicated in multiple molecular processes as cell cycle, apoptosis, and cell proliferation, so this miRNA has been proposed as a putative therapeutic target.²³ *CCND2* is an *miR-494* putative target and is essential for the control of the cell cycle at the G₁ to S transition.⁴⁰

Although the results of this study warrant functional validation, our findings suggest that the miRNA signature is related to the gene expression profile in NMZL in several ways. For instance, the up-regulation of *miR-223* and *miR-221*, which target the GC-related genes *LMO2* and *CD10*, could be partially responsible for the expression of a marginal zone signature. Similarly, the most up-regulated miRNAs in the signature showed a significant positive correlation (Pearson GSEA analysis) with important B-cell pathways, such as *BCR*, *IL2*, *IL6*, *CD40*, *NF-κB*, *TGFβ*, and memory B cells. These pathways were also found in the GSEA analysis (NMZL vs RLN comparison), suggesting a significant role for these pathways in NMZL.

Even though deletions of the chromosomal band 6q21-q25 involving the *NF-κB* negative regulator *TNFAIP3* (*A20*) have been described as characteristic cytogenetic abnormalities for MZLs,⁴⁻⁶ we were unable to confirm this finding in our series (Figure 6; supplemental Table 5; supplemental Figure 3). This could be a consequence of the small number of cases studied or the resolution of the CGH arrays used for each study.

In conclusion, this analysis shows that the NMZL gene expression profile reproduces the signature of normal marginal zone and memory B cells, identifies *BCR* signaling, interleukins (*IL2*, *IL6*, *IL10*), integrins (*CD40*), and survival pathways (*MAPKs*, *TNF*,

TGFβ, *NF-κB*) as the most significant pathways in NMZL pathogenesis, and allows new specific markers (*TACI*, *CHIT1*, *CD44*, *CD82*, *TGFβ1*, *miR-223*, *let-7f*, and *miR-221*) to be proposed as a means of distinguishing this lymphoma type from FL. Our study also identifies some possible therapeutic targets, such as *TACI* and *CD74*.

Acknowledgments

The authors thank R. Diaz de Otazu (Vitoria), C. Lobo (San Sebastián), S. Nieto (Madrid), P. Domínguez (Madrid), J. San Juan (Valencia), P. Navarro (Valencia), J. Escobar Jario (Asturias), and Laura Cereceda (Spanish National Cancer Research Center Tumor Bank) for kindly providing the cases included in this series and S. Opazo, Y. Ruano, and B. Meléndez (HVS) for their excellent technical help.

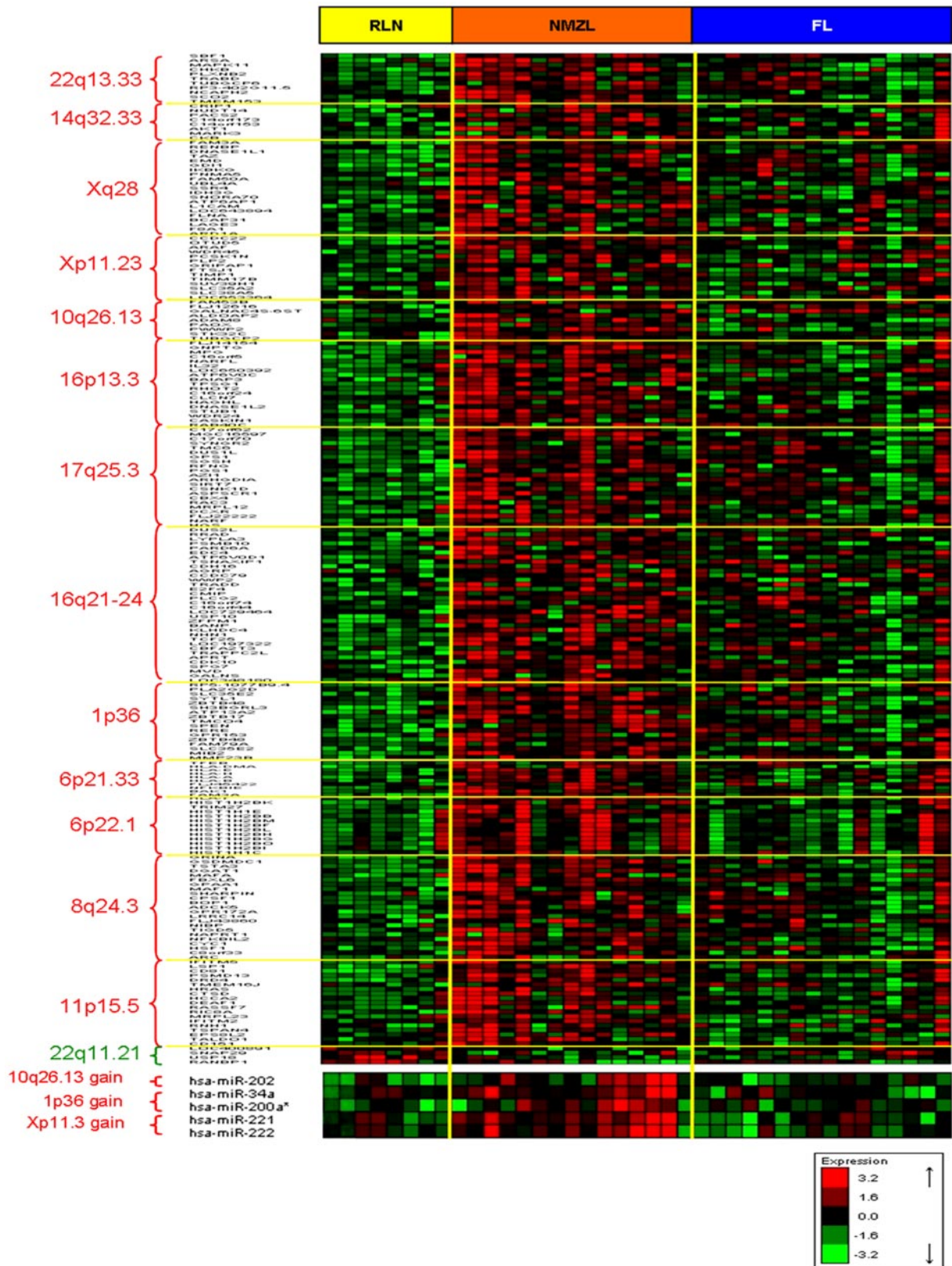
This work was supported by the Ministerio de Sanidad y Consumo (RETICS, FIS PI052742, PI081666, PI052800, and INT09/276), Ministerio de Ciencia e Innovación (SAF2008-03871), the Servicio de Salud de Castilla la Mancha (FISCAM PI2008/31), and the Asociación Española Contra el Cáncer.

Authorship

Contribution: A.J.A. analyzed microarray data, performed research, and wrote the paper; Y.C.-M. and P.A. analyzed data and performed research; C.G.-A. analyzed CGH data and performed research; M.S.-B. performed research and contributed analytical tools; M.S.R.-P. performed research and reviewed cases; S.M.-M. and J.A.-F. performed research and contributed samples; and M.A.P. and M.M. designed the study.

Conflict-of-interest disclosure: The authors declare no competing financial interests.

Correspondence: Manuela Mollejo, Avda Barber 30, CP 45004, Toledo, Spain; e-mail: mmollejov@sescam.jccm.es.



Downloaded from http://ashpublications.net/blood/article-pdf/119/3/e9/1464583/zh8003120000e9.pdf by guest on 29 May 2024

Figure 7. CNA, GEP and miRNA integration data. Hierarchical clustering of signature genes located in the chromosomal bands with copy number aberrations. Red and green represent high- and low-level expression, respectively.

References

1. Swerdlow SH, Campo E, Harris NL, et al. *WHO Classification of Tumours of Haematopoietic and Lymphoid Tissues*. Lyon, France: International Agency for Research on Cancer; 2008.

2. Ott G, Katzenberger T, Greiner A, et al. The t(11;18)(q21;q21) chromosome translocation is a

- frequent and specific aberration in low-grade but not high-grade malignant non-Hodgkin's lymphomas of the mucosa-associated lymphoid tissue (MALT-) type. *Cancer Res.* 1997;57(18):3944-3948.
3. Mateo M, Mollejo M, Villuendas R, et al. 7q31-32 allelic loss is a frequent finding in splenic marginal zone lymphoma. *Am J Pathol.* 1999;154(5):1583-1589.
 4. Novak U, Rinaldi A, Kwee I, et al. The NF- κ B negative regulator TNFAIP3 (A20) is inactivated by somatic mutations and genomic deletions in marginal zone lymphomas. *Blood.* 2009;113(20):4918-4921.
 5. Kato M, Sanada M, Kato I, et al. Frequent inactivation of A20 in B-cell lymphomas. *Nature.* 2009;459(7247):712-716.
 6. Rinaldi A, Mian M, Chigrinova E, et al. Genome-wide DNA profiling of marginal zone lymphomas identifies subtype-specific lesions with an impact on the clinical outcome. *Blood.* 2011;117(5):1595-1604.
 7. Kanellis G, Roncador G, Arribas A, et al. Identification of MND1 as a new marker for nodal marginal zone lymphoma. *Leukemia.* 2009;23(10):1847-1857.
 8. Piris MA, Rivas C, Morente M, Cruz MA, Rubio C, Oliva H. Monocytoid B-cell lymphoma, a tumour related to the marginal zone. *Histopathology.* 1988;12(4):383-392.
 9. Spencer J, Perry ME, Dunn-Walters DK. Human marginal-zone B cells. *Immunol Today.* 1998;19(9):421-426.
 10. Shen Y, Iqbal J, Xiao L, et al. Distinct gene expression profiles in different B-cell compartments in human peripheral lymphoid organs. *BMC Immunol.* 2004;5:20.
 11. Montes-Moreno S, Roncador G, Maestre L, et al. Gcet1 (centerin), a highly restricted marker for a subset of germinal center-derived lymphomas. *Blood.* 2008;111(1):351-358.
 12. Ruiz-Ballesteros E, Mollejo M, Rodriguez A, et al. Splenic marginal zone lymphoma: proposal of new diagnostic and prognostic markers identified after tissue and cDNA microarray analysis. *Blood.* 2005;106(5):1831-1838.
 13. Huynh MQ, Wacker HH, Wundisch T, et al. Expression profiling reveals specific gene expression signatures in gastric MALT lymphomas. *Leuk Lymphoma.* 2008;49(5):974-983.
 14. Basso K, Sumazin P, Morozov P, et al. Identification of the human mature B cell miRNome. *Immunity.* 2009;30(5):744-752.
 15. Jima DD, Zhang J, Jacobs C, et al. Deep sequencing of the small RNA transcriptome of normal and malignant human B cells identifies hundreds of novel microRNAs. *Blood.* 2010;116(23):e118-e127.
 16. Zhang J, Jima DD, Jacobs C, et al. Patterns of microRNA expression characterize stages of human B-cell differentiation. *Blood.* 2009;113(19):4586-4594.
 17. Rodríguez A, Villuendas R, Yáñez L, et al. Molecular heterogeneity in chronic lymphocytic leukemia is dependent on BCR signaling: clinical correlation. *Leukemia.* 2007;21(9):1984-1991.
 18. Ach RA, Wang H, Curry B. Measuring microRNAs: comparisons of microarray and quantitative PCR methods, and of different total RNA prep methods. *BMC Biotechnol.* 2008;8:69.
 19. Ferreira BI, Garcia JF, Suela J, et al. Comparative genome profiling across subtypes of low-grade B-cell lymphoma identifies type-specific and common aberrations that target genes with a role in B-cell neoplasia. *Haematologica.* 2008;93(5):670-679.
 20. Aggarwal M, Sánchez-Beato M, Gómez-López G, et al. Functional signatures identified in B-cell non-Hodgkin lymphoma profiles. *Leuk Lymphoma.* 2009;50(10):1699-1708.
 21. Liva S, Hupé P, Neuvial P, et al. CAPweb: a bioinformatics CGH array Analysis Platform. *Nucleic Acids Res.* 2006;34(Web Server issue):W477-W481.
 22. Di Lisio L, Gómez-López G, Sánchez-Beato M, et al. Mantle cell lymphoma: transcriptional regulation by microRNAs. *Leukemia.* 2010;24(7):1335-1342.
 23. Barh D, Malhotra R, Ravi B, Sindhurani P. MicroRNA let-7: an emerging next-generation cancer therapeutic. *Curr Oncol.* 2010;17(1):70-80.
 24. Weill JC, Weller S, Reynaud CA. Human marginal zone B cells. *Annu Rev Immunol.* 2009;27:267-285.
 25. Chng WJ, Remstein ED, Fonseca R, et al. Gene expression profiling of pulmonary mucosa-associated lymphoid tissue lymphoma identifies new biologic insights with potential diagnostic and therapeutic applications. *Blood.* 2009;113(3):635-645.
 26. Herreros B, Sanchez-Aguilera A, Piris M. Lymphoma microenvironment: culprit or innocent? *Leukemia.* 2008;22(1):49-58.
 27. Stein R, Mattes M, Cardillo T, et al. CD74: a new candidate target for the immunotherapy of B-cell neoplasms. *Clin Cancer Res.* 2007;13(18):5556s-5563s.
 28. Starlets D, Gore Y, Binsky I, et al. Cell-surface CD74 initiates a signaling cascade leading to cell proliferation and survival. *Blood.* 2006;107(12):4807-4816.
 29. Mantchev GT, Cortesao CS, Rebrovich M, Cascalho M, Bram RJ. TAC1 is required for efficient plasma cell differentiation in response to T-independent type 2 antigens. *J Immunol.* 2007;179(4):2282-2288.
 30. He B, Chadburn A, Jou E, Schattner EJ, Knowles DM, Cerutti A. Lymphoma B cells evade apoptosis through the TNF family members BAFF/BLyS and APRIL. *J Immunol.* 2004;172(5):3268-3279.
 31. Zandvoort A, Timens W. The dual function of the splenic marginal zone: essential for initiation of anti-TI-2 responses but also vital in the general first-line defense against blood-borne antigens. *Clin Exp Immunol.* 2002;130(1):4-11.
 32. Kim S, Letterio J. Transforming growth factor-beta signaling in normal and malignant hematopoiesis. *Leukemia.* 2003;17(9):1731-1737.
 33. Wrzesinski SH, Wan YY, Flavell RA. Transforming growth factor-beta and the immune response: implications for anticancer therapy. *Clin Cancer Res.* 2007;13(18):5262-5270.
 34. Marasca R, Vaccari P, Luppi M, et al. Immunoglobulin gene mutations and frequent use of VH1-69 and VH4-34 segments in hepatitis C virus-positive and hepatitis C virus-negative nodal marginal zone B-cell lymphoma. *Am J Pathol.* 2001;159(1):253-261.
 35. Cocquerel L, Kuo C, Dubuisson J, Levy S. CD81-dependent binding of hepatitis C virus E1E2 heterodimers. *J Virol.* 2003;77(19):10677-10683.
 36. Zarnegar BJ, Wang Y, Mahoney DJ, et al. Noncanonical NF-kappaB activation requires coordinated assembly of a regulatory complex of the adaptors cIAP1, cIAP2, TRAF2 and TRAF3 and the kinase NIK. *Nat Immunol.* 2008;9(12):1371-1378.
 37. Shi X, Leng L, Wang T, et al. CD44 is the signaling component of the macrophage migration inhibitory factor-CD74 receptor complex. *Immunity.* 2006;25(4):595-606.
 38. Malaguamera L, Musumeci M, Di Rosa M, Scuto A, Musumeci S. Interferon-gamma, tumor necrosis factor-alpha, and lipopolysaccharide promote chitotriosidase gene expression in human macrophages. *J Clin Lab Anal.* 2005;19(3):128-132.
 39. Wada K, Maeda K, Tajima K, Kato T, Kobata T, Yamakawa M. Expression of BAFF-R and TAC1 in reactive lymphoid tissues and B-cell lymphomas. *Histopathology.* 2009;54(2):221-232.
 40. Huang W, Chang HY, Fei T, Wu H, Chen YG. GSK3 beta mediates suppression of cyclin D2 expression by tumor suppressor PTEN. *Oncogene.* 2007;26(17):2471-2482.